

Learning Robust Motion Skills via Critical Adversarial Attacks for Humanoid Robots

Yang Zhang¹, Zhanxiang Cao², Buqing Nie², Haoyang Li¹ and Yue Gao^{3†}

Abstract—Humanoid robots show significant potential in daily tasks. However, reinforcement learning-based motion policies often suffer from robustness degradation due to the sim-to-real dynamics gap, thereby affecting the agility of real robots. In this work, we propose a novel robust adversarial training paradigm designed to enhance the robustness of humanoid motion policies in real worlds. The paradigm introduces a learnable adversarial attack network that precisely identifies vulnerabilities in motion policies and applies targeted perturbations, forcing the motion policy to enhance its robustness against perturbations through dynamic adversarial training. We conduct experiments on the Unitree G1 humanoid robot for both perceptive locomotion and whole-body control tasks. The results demonstrate that our proposed method significantly enhances the robot’s motion robustness in real world environments, enabling successful traversal of challenging terrains and highly agile whole-body trajectory tracking.

I. INTRODUCTION

Humanoid robots, with their human-like morphology and versatile mobility [1], have the potential to replace humans in performing various tasks in daily life [2], demonstrating significant potential in fields such as domestic service [3], industrial production [4], and healthcare [5]. Robust motion control of humanoid robots is the basis for achieving other complex tasks [6]. In scenarios such as carrying objects [7] and performing high-precision operations [1], robots must have the ability to move autonomously and maintain body balance in dynamic unknown terrain environments [8]. Furthermore, robots need to adapt to external disturbances during interactions with the environment [9], such as unexpected collisions or slippage of feet, to prevent falls and ensure task safety [10]. However, the high Degrees of Freedom (DoF) and the complex kinematic coupling between the upper-body and lower-body make the development of flexible and stable locomotion control systems highly challenging [11], limiting their broader deployment in real world applications [12].

Traditional model-based control methods are based on precise dynamic modeling and complex parameter tuning [13]. However, these methods struggle to comprehensively capture the diversity and complexity of humanoid robot interactions with the environment [14], leading to degraded control



Fig. 1. Snapshot of the humanoid robot executing whole-body trajectory tracking. PL-CAP can track challenging dynamic trajectories over an extended duration, demonstrating that adversarial training based on critical attacks significantly improves the robustness of motion policies.

performance or even failure in complex terrain environments [1]. Recently, with the rapid development of simulation technology and computing power, Reinforcement Learning (RL)-based locomotion control has emerged as a promising alternative [15]–[17]. By learning the optimal policy through interaction with the environment in simulation, the robot can autonomously adapt and optimize its motion behavior in complex environments [12], [18]. The trained policy is then transferred from the simulation to the real robot to achieve flexible motion capabilities [19], [20]. However, due to the discrepancies between the simulation environment and the real environment [21], including environmental variations [22], sensor noise [23], and external disturbances [24], neural controllers are likely to encounter domain distribution shifts [22], leading to the sim-to-real transfer problem of motion policies [25]. Additionally, the inherent sensitivity of RL-based neural controllers to perturbations further exacerbates the instability of deploying these policies in real world applications [26].

To enhance the robustness of motion policies on real robots, prior works have employed domain randomization [11] to reduce the distribution gap between simulated and real world data, thereby improving the robustness of the policy to environmental uncertainty [15]. However, domain randomization fails to precisely identify specific vulnerability

¹Yang Zhang and Haoyang Li are with Department of Automation, Shanghai Jiao Tong University, Shanghai, P.R. China. Email: zhangyang-sjtu-2022@sjtu.edu.cn, Lhy_0415@sjtu.edu.cn

²Zhanxiang Cao and Buqing Nie are with Department of Computer Science, Shanghai Jiao Tong University, Shanghai, P.R. China. Email: caozx1110@sjtu.edu.cn, niebuqing@sjtu.edu.cn

³Yue Gao is with MoE Key Lab of Artificial Intelligence and AI Institute, Shanghai Jiao Tong University, Shanghai, P.R. China. Email: yuegao@sjtu.edu.cn

† Corresponding author.

of neural policies and is difficult to generate high-quality perturbations samples to assist policy training [18], [27]. Furthermore, excessive domain randomization can significantly degrade policy performance [28]. In contrast, adversarial attacks introduce carefully designed perturbations that severely degrade neural network performance [25], effectively identifying network vulnerabilities and evaluating the robustness of motion policies [29]. Additionally, adversarial training incorporates adversarial samples into the training data to enhance the ability of motion policies to resist perturbations and improve the robustness of motion policies in real environments [30]–[32].

In this paper, we propose a novel robust adversarial training paradigm to enhance the robustness of humanoid motion policies in real world environments. This paradigm introduces a learnable adversary network to identify potential vulnerabilities in motion policies and assist in optimizing the policy to improve the robot’s ability to resist perturbations. The attacker is designed to identify vulnerabilities in humanoid motion states and apply targeted perturbation attacks, aiming to destabilize the robot with minimal attack cost. Through a non-zero-sum adversarial training framework, we alternately optimize attack policies and motion policies, enhancing the attacker’s ability to generate effective perturbations while progressively improving the motion policy’s robustness against such perturbations. We conduct extensive experiments on the Unitree G1 humanoid robot [33] in various challenging terrains and agile trajectory tracking. The results demonstrate that our approach significantly improves the motion performance of humanoid robots in real world environments.

In summary, the contributions of this work are as follows:

- A novel robust adversarial training paradigm for humanoid robots is proposed. By introducing adversarial attack policies to identify vulnerabilities of motion policies, effective adversarial samples are generated to enhance the robustness of motion policies.
- The critical attack policy is proposed by constraining attack costs. It improves the vulnerability mitigation of motion policies rather than conservative degradation.
- Extensive experimental results demonstrate that our method effectively enhances the robustness of motion policies and significantly improves the motion performance of the real robot.

II. RELATED WORK

A. Learning-Based Humanoid Motion Control

In recent years, RL-based approaches have achieved impressive results in humanoid robot motion control [6], [11], [16], [34], [35], especially in complex terrain traversal [17], [18] and whole-body trajectory imitation [9], [36]. These methods narrow the gap between simulation and reality through reward shaping [15], [19], reference trajectory guidance [21], [37], and robustness constraints [10], thereby improving the performance of motion policies when applied to real robots. For instance, [6], [35] and [38] employ

encoder-decoder architectures to learn accurate state estimation. Wang et al. [39] further utilize saliency analysis to quantitatively evaluate the impact of different state information on the performance of motion policies. The adversarial motion priors (AMP) approach encourages generated motion trajectories to align with human motion characteristics [8], thereby eliminating the need for laborious auxiliary reward engineering [40]. Radosavovic et al. [16] use causal transformers trained via autoregressive modeling of observations and actions on diverse motion datasets, achieving stable long-distance walking in outdoor environments. [18], [41] and [42] extract terrain features around the robot based on visual perception information to enhance the robot’s locomotion capabilities in challenging unstructured terrains, enabling humanoid parkour [17]. Chen et al. [12] improve action smoothness and policy transfer robustness based on Lipschitz constraints. Marum et al. [19] construct benchmark test environments to systematically evaluate the performance of diverse motion policies. Furthermore, by remapping human motion trajectories from teleoperation and motion capture (MoCap) to humanoid robots [20], [43], whole-body imitation learning frameworks have been developed to replicate expressive human-like movements [44]. However, the high dynamicity of whole-body motions exacerbates the sim-to-real gap, significantly compromising robot stability [45]. He et al. [46] compensate for dynamic mismatches by collecting data in real robots to train a residual action model and incorporate it in simulation to fine-tuning policy for align with real-world dynamics. In contrast to the aforementioned approaches, this work focuses on the vulnerability of neural controllers under perturbations. We investigate attack methods to identify security vulnerabilities in controllers, and subsequently leverage these adversarial samples to enhance the robustness of motion policies against perturbations.

B. Robust Reinforcement Learning

Robust adversarial training introduces adversarial attacks during training [25], allowing the agent to learn under uncertain perturbations and improve its robustness in real environments [29]. Adversarial attacks can impose perturbations in the observation space [30], action space [31], reward space [47], and environmental state space [32], effectively simulating various uncertainties that the task policy may encounter in deployment scenarios. Shi et al. [28] use adversarial attacks to evaluate the robustness of RL-based locomotion policies for quadrupedal robots and further improved the robustness of policies through adversarial samples. Long et al. [18] formulate robust locomotion policy learning for quadrupedal robots as a zero-sum game, while optimizing motion policy and external disturbance attacker, improving the performance of the quadruped robot in resisting external disturbances. [48] decouples the upper-body and lower-body control of humanoid robots as two independent agents, proposing an adversarial motion and imitation learning framework. This approach facilitates adversarial policy learning between upper-body trajectory tracking and lower-body velocity tracking, thereby significantly improving

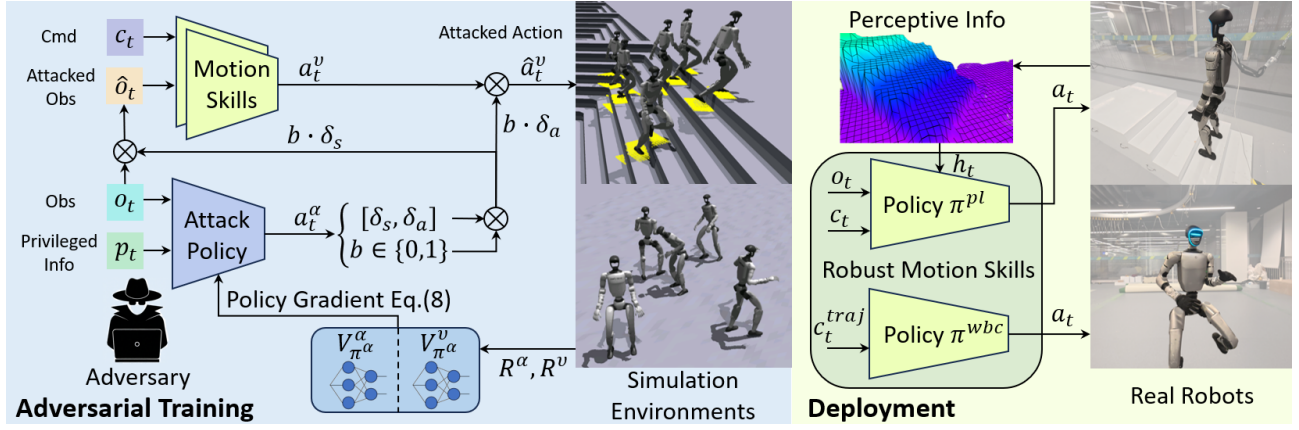


Fig. 2. Overview of the adversarial training framework. The CAP identifies vulnerabilities in motion states and generates adversarial samples by applying perturbations in both state space and action space. Through alternating adversarial training under non-zero-sum game, the motion policy continuously addresses its own vulnerabilities using adversarial samples, thereby enhancing its robustness against perturbations. During deployment, the robust motion skills are deployed to real-world robots without requiring attack policies, enabling robust whole-body motion control for humanoid robots

robotic stability. On the other hand, considering the high sensitivity of neural networks to small input perturbations [49], some studies have investigated the use of Lipschitz-constrained policy networks [50] to enhance robustness against input noise and small perturbations [26]. By regularizing or employing specialized network architectures to constrain the Lipschitz constant of neural networks [51], the output actions of the policy can be effectively smoothed [52], thereby improving the robustness of the policy to perturbations [12]. This work develops critical attack policy to identify vulnerable states in humanoid motion policy deployment, applies targeted adversarial perturbations, and constructs a robust adversarial training framework based on non-zero-sum games. This approach significantly enhances the robustness of robotic motion policies, demonstrating measurable performance improvements across various motion skills in real robots.

III. PRELIMINARIES

A. Reinforcement Learning

The RL-based control problem is usually formulated as a Markov Decision Process (MDP), where an agent π dynamically interacts with the environment through trial-and-error mechanisms to maximize the task-specific objective function. The MDP is defined as $\mathcal{M} = (\mathcal{S}, \mathcal{A}, \mathcal{P}, R, \gamma)$, where \mathcal{S} is the state space, \mathcal{A} is the action space, $\mathcal{P} : \mathcal{S} \times \mathcal{A} \times \mathcal{S} \rightarrow \mathbb{R}$ is the transition probability, $R(s, a)$ is the reward function, and $\gamma \in [0, 1)$ is the discount factor. At each timestep t , the agent π receives an observation s_t and chooses an action $a_t \in \pi(s_t)$ to obtain the reward $R(s_t, a_t)$. The agent's goal is to maximize the expected cumulative return:

$$J(\pi) = \mathbb{E}_{\pi} \left[\sum_{t=0}^{\infty} \gamma^t R(s_t, a_t) \right]. \quad (1)$$

B. Adversarial Training as Two-player Markov Game

A two-player Markov game [53] can be formally represented as $(\mathcal{N}, \mathcal{S}, \{\mathcal{A}^i\}_{i \in \mathcal{N}}, \mathcal{T}, \{R^i\}_{i \in \mathcal{N}}, \gamma)$, where $\mathcal{N} =$

$\{\pi^\alpha, \pi^v\}$ represents the set of agents with adversary π^α and victim π^v . \mathcal{S} represents the state space of the global environment observations. \mathcal{A}^i represents the action space of the agent i . $\mathcal{T} : \mathcal{S} \times \mathcal{A}^\alpha \times \mathcal{A}^v \rightarrow \mathbb{R}$ represents the transition probability for any joint actions of both agents. $R^i : \mathcal{S} \times \mathcal{A} \rightarrow \mathbb{R}$ is the reward function for the agent i . γ is the discount factor. The state-value function for each agent is defined as a function of the joint policy $\pi(a|s) = \prod_{\pi^i \in \mathcal{N}} \pi^i(a^i|s)$

$$V_{\pi}^i(s) = \mathbb{E}_{a \sim \pi(a|s)} [R^i(s, a) + \gamma \mathbb{E}_{s' \sim \mathcal{T}} [V_{\pi}^i(s')]]. \quad (2)$$

In this Markov game, the victim π^v improves its defense capability by maximizing its state value function $V_{\pi}^v(s)$, while the adversary π^α enhances its attack effect by maximizing its state value function V_{π}^α , thereby enhancing the adversarial robustness.

IV. METHODS

In this section, we present in detail the adversarial training method designed to enhance the robustness of humanoid motion policies through critical adversarial attacks. As illustrated in Fig. 2, the framework comprises two learnable modules: motion policy and adversarial attack policy. The motion policy is trained to optimize motion task performance in an environment perturbed by the adversarial attack policy, thereby improving its resilience against perturbations. In contrast, the adversarial attack policy learns to identify vulnerable states of the robot through environmental state observations and selectively applies critical adversarial perturbations to force the robot into falling states. During the training process, these two modules are alternately optimized in a game-theoretic manner, forming a dynamic equilibrium learning process. The adversarial attack policy progressively improves its ability to identify vulnerabilities in the motion policy and generate effective perturbations, while the motion policy continuously compensates for its weaknesses to strengthen its robustness against perturbations.

A. Learning Critical Adversarial Attacks

When RL-based neural controllers are applied to humanoid robots, the observed states acquired through sensors are susceptible to natural observation noise and outliers, causing deviations from the true states. This discrepancy leads the policy to generate suboptimal actions. Furthermore, tracking latency in actuator responses and mechanical wear-induced errors introduce significant execution deviations in the policy’s output actions, thereby substantially degrading the robot’s motion performance. To comprehensively identify vulnerabilities in motion policies caused by observation and actuator errors, we define the action space of adversarial attack policy as the joint space of the motion policy state space and action space. Unlike previous works that focus only on single-space attacks (e.g., perturbations of state-only or action-only), joint attacks operating on both state and action spaces can more comprehensively evaluate the vulnerability of policies in actual robotic systems.

Let $\mathcal{B}_s = \{s + \delta_s | \delta_s \in \mathcal{D}_s\}$ and $\mathcal{B}_a = \{a + \delta_a | \delta_a \in \mathcal{D}_a\}$ be bounded perturbation sets for states and actions, respectively, where $\|\delta_s\| \leq \epsilon_s$, $\|\delta_a\| \leq \epsilon_a$. Given a pre-trained motion policy π^m on MDP $\mathcal{M} = (\mathcal{S}, \mathcal{A}, P, R, \gamma)$, we construct an adversarial MDP $\hat{\mathcal{M}} = (\mathcal{S}, \hat{\mathcal{A}}, \hat{P}, \hat{R}, \gamma)$ where $\hat{\mathcal{A}} = \mathcal{S} \times \mathcal{A}$ represents the joint state-action attack space, $\hat{P}(s'|s, \hat{a}) = \mathbb{E}_{a \sim \pi^m(\cdot | s + \delta_s)}[\mathcal{P}(s'|s, a + \delta_a)]$, and $\hat{R}(s, a)$ encodes attack objectives. The adversarial attack policy π^{adv} in $\hat{\mathcal{M}}$ maximizes attack efficacy while satisfying perturbation bounds $\mathcal{B}_s, \mathcal{B}_a$.

Due to its temporal homogeneity, the Persistent Attack Policy (PAP) derived from the above method presents two key limitations in enhancing the robustness of motion policies: (1) Insufficient Vulnerability Identification. This uniform temporal distribution of perturbations violates the sparse criticality principle observed in humanoid motion, which cannot effectively distinguish the vulnerability differences between different states of the robot, resulting in the dispersion of attack energy in the robust state, while the key vulnerable state is not targeted. (2) Detectability-Induced Conservative Degradation. This indiscriminate attack pattern makes it easy to identify the state distribution shift ($\mathcal{P}_S \rightarrow \mathcal{P}_{S'}$) caused by the PAP when the motion policy is further optimized under the disturbance of the PAP, and learn to impose active security defense decisions, resulting in the degradation of conservative strategies rather than real vulnerability mitigation.

To address these limitations, we propose a Critical Attack Policy (CAP), which not only determines how to generate optimal perturbations, but also identifies the critical states where attacks will be most effective. To achieve stealthy and efficient adversarial influence, CAP aims to significantly degrade the performance of motion policy using only a minimal number of attack steps, thereby maximizing impact while minimizing detectability. In an episode, the motion policy produces a state-action sequence $\{s_t, a_t\}_{t=0}^T$. The CAP strategically selects a subset of timesteps $\mathcal{T}_{adv} \subset \{1, \dots, T\}$ (where $|\mathcal{T}_{adv}| \ll T$) to perturb the robot, rather

than attacking all timesteps. Let $\{\delta_1, \dots, \delta_T\}$ denote a sequence of perturbations sampled from an arbitrary attack policy π^{adv} , and N_a be the attack budget. The CAP can be formulated as the following optimization problem:

$$\begin{aligned} \max_{b_0, \dots, b_T, \pi^{adv}} \quad & \mathbb{E}\left[\sum_{t=0}^T \hat{R}(s_t, a_t)\right] \\ \text{s.t.} \quad & [\delta_s, \delta_a] \sim \pi^{adv}(s_t), \\ & a_t \sim \pi(s_t + b_t \delta_{s,t} + b_t \delta_{a,t}), \\ & s_{t+1} \sim \mathcal{P}(s_t, a_t), \\ & \sum_{t=0}^T b_t \leq N_a. \end{aligned} \quad (3)$$

The binary variable b_t indicates whether the perturbation $\pi^{adv}(s_t)$ is added to the state s_t , and step t is a critical step found by the CAP if $b_t = 1$. To address the attack budget constraint in problem (3), we introduce a Lagrange multiplier λ to transform the hard budget constraint into a soft penalty term:

$$\max_{b_0, \dots, b_T, \pi^{adv}} \quad \mathbb{E}\left[\sum_{t=0}^T \hat{R}(s_t, a_t)\right] - \lambda \sum_{t=0}^T b_t. \quad (4)$$

The λ is a hyperparameter that controls the penalty for each attack. A higher penalty parameter λ corresponds to a lower budget constraint N_a . We use RL to train CAP in another MDP $\hat{\mathcal{M}}' = (\mathcal{S}, \hat{\mathcal{A}}', \hat{P}', \hat{R}', \gamma')$, where $\hat{\mathcal{A}}' = \{0, 1\} \times \hat{\mathcal{A}}$, $\hat{P}'(s'|s, \hat{a}') = \mathbb{E}_{a \sim \pi^m(\cdot | s + b\delta_s)}[\mathcal{P}(s'|s, a + b\delta_a)]$, $\hat{R}' = \hat{R} - \lambda b$, and $\gamma' = 1$.

B. Enhancing Policy Robustness via Adversarial Training

Under the adversarial training framework defined in Section III-B, the reward function $R^\alpha = -R^v$ establishes a zero-sum game between the victim π^α and the adversary π^v , where both policy updates follow an iterative competitive process to maximize and minimize the shared value function, respectively. As demonstrated by Perolat et al. [54], the optimal equilibrium value function ensures the equivalence between the minimax equilibrium and the Nash equilibrium in such games:

$$V_{\pi^*}^\alpha(s) = \min_{\pi^v} \max_{\pi^\alpha} V_{\pi^\alpha}^\alpha(s) = \max_{\pi^\alpha} \min_{\pi^v} V_{\pi^\alpha}^\alpha(s). \quad (5)$$

However, previous analyses of the minimax formulation in adversarial training shows that the attacker learned under the zero-sum game framework does not guarantee continuous improvement in attack performance. This results in a weak adversary dilemma, which in turn leads to a robust overfitting of the victim.

In this work, we formulate the adversarial training between the motion policy π^m and the attack policy π^{adv} as a non-zero-sum game. The attack policy maximizes the attack reward R^{adv} associated with the robot’s safety failure while negatively affecting the motion policy, which can be formally expressed as:

$$J(\theta_{adv}) = \underset{\theta_{adv}}{\text{maximize}} (V_{\pi^m}^{adv}(s) - V_{\pi^m}(s)), \quad (6)$$

Algorithm 1 Alternating Adversarial Training

Input: Initialize the motion policy π^m with pre-trained parameters θ_m , initialize the attack policy with random parameters θ_{adv} , environment \mathcal{E} , batch size B .

```
1: for  $i = 1$  to  $N_{iter}$  do
2:   for  $j = 1$  to  $N_{adv}$  do
3:      $\{(s_t, a_t^m, a_t^{adv}, R_t^m, R_t^{adv})\} \leftarrow \text{rollout}(\mathcal{E}, \pi^m, \pi^{adv}, B)$ 
4:     Update  $\theta_{adv}$  with  $\mathcal{D}_{adv} := \{(s_t, a_t^{adv}, R_t^m, R_t^{adv})\}$ 
5:   end for
6:   for  $j = 1$  to  $N_m$  do
7:      $\{(s_t, a_t^m, a_t^{adv}, R_t^m, R_t^{adv})\} \leftarrow \text{rollout}(\mathcal{E}, \pi^m, \pi^{adv}, B)$ 
8:     Update  $\theta_m$  with  $\mathcal{D}_m := \{(s_t, a_t^m, R_t^m)\}$ 
9:   end for
10: end for
```

where θ_{adv} is the parameter of the attack policy network, $V_{\pi}^{adv}(s)$ and $V_{\pi}^m(s)$ represent the attacker’s value function and the motion agent’s value function, respectively. A trivial solution to solving Eq. (6) involves applying policy gradient methods. However, this solution does not guarantee monotonic changes in both value functions. Taking advantage of the work [53], a new optimization objective that can guarantee the monotonicity of Eq. (6) is obtained by approximating the value function:

$$\begin{aligned} & \underset{\theta_{adv}}{\operatorname{argmax}} \mathbb{E}_{(a_t^{adv}, s_t) \sim \pi_k^{adv}} [\min(\operatorname{clip}(\rho_t, 1 - \epsilon, 1 + \epsilon) A_t^{adv}, \\ & \quad \rho_t A_t^{adv}) - \min(\operatorname{clip}(\rho_t, 1 - \epsilon, 1 + \epsilon) A_t^m, \rho_t A_t^m)], \\ \rho_t &= \frac{\pi^{adv}(a_t^{adv} | s_t)}{\pi_k^{adv}(a_t^{adv} | s_t)}, A_t^{adv} = A_{\pi_k^{adv}}^{adv}(a_t^{adv}, s_t), \\ A_t^m &= A_{\pi_k^{adv}}^m(a_t^{adv}, s_t), \end{aligned} \quad (7)$$

where π_k^{adv} denotes the old attack policy and ϵ represents the clipping parameter in the PPO algorithm. Subsequently, we employ temporal difference learning with two separate neural networks to approximate the value functions of the attack policy and the motion policy. The policy gradient method is then applied to optimize Eq. (7), learning a powerful attack policy.

We employ an alternating training procedure to optimize the motion policy and the attack policy. Algorithm 1 outlines our approach in detail. The motion policy is initialized from the pre-trained policy, while the attack policy is randomly initialized. In N_{adv} iterations, the motion policy is fixed and embedded into the environment, and the attack policy is optimized to find the intrinsic weaknesses of the motion policy and impose attacks. Then in N_m iterations, the attack policy is fixed, enabling the motion policy to be further optimized for resilience against adversarial attacks. Through dynamic alternating optimization over N_{iter} iterations, our framework achieves online robust adversarial training. This paradigm promotes the motion policy to adaptively enhance its robustness against various adversarial attacks.

C. Implementation details

This paper applies critical adversarial attacks to two motion skills learning frameworks: perceptive locomotion and whole-body control of humanoid robots, thereby achieving robust adversarial training to further enhance the robustness of motion policies. All policies are modeled using neural networks and trained using the PPO algorithm.

1) *Learning Robust Perceptive Locomotion:* We train a velocity-command-tracking locomotion policy on the Unitree G1 humanoid robot (29 DoF), leveraging a LiDAR-based elevation map for unstructured terrain perception. In Isaac Gym, an asymmetric actor-critic structure is employed to estimate privileged information from historical observations, which is then fed into the policy network, enabling single-stage policy learning without distillation. We sample 121 elevation points within the Z-axis-aligned robot frame in the simulation. These points are distributed across a $1.0m \times 1.0m$ square centered on the robot, and their deviations from the mean value are used as the perceptive input h_t for the locomotion policy. The elevation map module, deployed via Mid-360 LiDAR on the real robot, ensures consistency between real-world observations and the simulated perceptive information. The locomotion policy’s observation $o_t = [c_t, \omega_t, g_t, q_t, \dot{q}_t, a_{t-1}, h_t]$ contains velocity command $c_t = [v_x^c, v_y^c, \omega_{yaw}^c]$, base angular velocity ω_t , gravity projection g_t , joint position q_t , joint velocity \dot{q}_t , last timestep action a_{t-1} , and perceptive information h_t . The critic is allowed to access additional privileged information such as base linear velocity v_t and other environmental parameters. The locomotion policy outputs target joint positions, which are subsequently converted to joint torques through PD controllers. The reward function design is consistent with that in [42], which mainly consists of velocity tracking rewards and regularization terms to make the policy output actions smoother and avoid constraint violations. Furthermore, to achieve more natural humanoid locomotion patterns, we incorporate an symmetry constraint loss \mathcal{L}_{sym} into the policy optimization process:

$$\mathcal{L}_{sym} = \operatorname{MSE}(\pi^m(s_t), M^a \cdot \pi^m(M^s \cdot s_t)), \quad (8)$$

where M^s and M^a represent the transformation matrices that mirror the state s_t and action a_t relative to the X-Z plane, respectively.

To effectively attack the locomotion policy, the CAP’s observation space comprises both the locomotion policy’s observations o_t and all privileged information. The action space of CAP is defined as:

$$a^{adv} = [\delta_{s1}, \delta_{s2}, \delta_{s3}, \delta_{a1}, \delta_{a2}, \delta_{a3}, \delta_{a4}] \times b, \quad (9)$$

which including additive attack δ_{s1} to the proprioceptive information, multiplicative attack δ_{s2} and additive attack δ_{s3} to the perceptive information h_t (formulated as $h_t^{attack} = \delta_{s2} \times h_t + \delta_{s3}$), additive attack δ_{a1} to the policy output action a_t , the K_P and K_D of the PD controller apply multiplicative attack δ_{a2} and δ_{a3} , respectively, multiplicative attack δ_{a4} to joint torques, and binary attack variable $b \in \{0, 1\}$. It should

be noted that we maintain consistency between our attack space and the perturbation space of previous work using DR, enabling direct experimental comparison to validate our method’s effectiveness. The adversarial reward function focuses exclusively on the robot’s stability metrics, which can be formally expressed as:

$$R^{adv} = c_1 \cdot \mathbb{1}_{fall} + c_2 \cdot (\theta_r^2 + \theta_p^2) + c_3 \cdot (\omega_x^2 + \omega_y^2) + c_4 \cdot v_z^2, \quad (10)$$

where $\mathbb{1}_{fall}$ denotes robot falling, θ_r and θ_p represent the base’s roll and pitch angles, respectively, ω indicates base angular velocity, and v indicates base linear velocity. The coefficients $c_i, i \in \{1, 2, 3, 4\}$ are weighting parameters. These terms collectively guide the adversarial attack policy to effectively attack the robot in unsafe states. Furthermore, to simulate more realistic perturbation characteristics in practical scenarios, we impose Lipschitz regularization on adversarial policy optimization [28]. By incorporating the infinite norm of the policy network parameters as a regularization loss term $\mathcal{L}_{lips} = \prod_{i=1} \|\theta_{adv}^i\|_\infty$ to constrain the Lipschitz constant of the network, thereby ensuring smoother adversarial attacks.

2) *Learning Robust Whole-Body Control*: We formulate the whole-body control problem as a target trajectory imitation learning task, where the imitation policy is trained to track the whole-body trajectory. The motion trajectories are derived from the open-source LAFAN1 dataset [55] and remapped to the Unitree G1 humanoid robot. Each trajectory includes the base position, the base quaternion, and all joint angles. We replay these trajectories in simulation and collect keyframe pose information of robot bodies to augment the reference trajectory information. Inspired by [20], the imitation policy takes $[o_t, c_t^{traj}]$ as input, and the output action a_t is converted into torque by the PD controller. The c_t^{traj} denotes the target trajectory frame at timestep t , represented in the robot’s local frame. The reward function follows the design of [20]. Similarly to Section IV-C.1, the symmetry constraint (8) is integrated into the imitation policy training framework.

In the design of adversarial policy against whole-body imitation policy, we exclude perceptive information attacks $[\delta_{s2}, \delta_{s3}]$ from the attack space designed in the Section IV-C.1, while all other training components (including the observation space and reward function) remain the same.

V. EXPERIMENTS

A. Experimental Setup

To systematically evaluate the effectiveness of the proposed adversarial training framework in enhancing the robustness of motion policies, this study applies it to two tasks of humanoid robots: Perceptive Locomotion (PL) and Whole-Body Control (WBC). Through comparative experiments and ablation studies, we address the following research questions: (1) Can the critical attack policy impose a stronger perturbation effect compared to domain randomization? (2) Does adversarial training further improve the robustness of motion policies? (3) Does adversarial training contribute to the motion performance of real robots?

TABLE I
TASK SUCCESS RATES UNDER DOMAIN RANDOMIZATION AND
ADVERSARIAL ATTACKS

Perturbation Mode	Motion Policies		
	PL/WBC-CE	PL/WBC-DR	PL/WBC-CAP
DR	77.3%	94.4%	97.4%
CAP	0.0%	0.0%	95.7%

1) *Baselines*: We design four different training settings for comparative analysis, and each motion policy is represented using the following notation:

- **PL/WBC-CE**: The motion policies trained in Clean Environments (CE), without domain randomization and adversarial attacks, serve as the baseline. Specifically, PL-CE represents the baseline of the perceptive locomotion policy, while WBC-CE represents the baseline of the whole-body control policy.
- **PL/WBC-DR**: Domain Randomization (DR) is added during the training process.
- **PL/WBC-PAP**: Adversarial training based on persistent attack policy.
- **PL/WBC-CAP (Ours)**: Adversarial training based on critical attack policy.

2) *Metrics*: We employ multiple metrics to evaluate the performance of motion policies. The mean linear velocity error $E_{vel}(m/s)$ and the mean angular velocity error $E_{ang}(rad/s)$ are used to evaluate the accuracy of velocity command tracking. The gravitational projection component $E_g(m/s^2)$ is utilized to evaluate the stability of robots. The Mean Per Keybody Position Error (MPKPE) for the upper body $E_{mpkpe}^{upper}(m)$ and the lower body $E_{mpkpe}^{lower}(m)$ evaluate the keypoint tracking of the upper body and the lower body, respectively. The Mean Per Joint Position Error (MPJPE) for the upper body $E_{mpjpe}^{upper}(rad)$ and the lower body $E_{mpjpe}^{lower}(rad)$ measure the joint tracking ability. The success rate $R_{sr}(\%)$ evaluates the survival rate of the robot to traverse complex terrain or track whole-body trajectories.

B. Simulation Results

1) *Effectiveness of Adversarial Perturbations*: To ensure the comparability of experimental results, we keep the domain randomization and attack policy with the same perturbation space and perturbation threshold during training. Subsequently, we evaluate the task success rates of motion policies learned under different training settings by separately applying domain randomization and adversarial attacks. As presented in Table I, domain randomization can significantly degrade the success rate of PL/WBC-CE, but has no effect on PL/WBC-CAP learned through adversarial training. Conversely, the critical attack policy can successfully attack both PL/WBC-CE and PL/WBC-DR. The experimental results show that simple domain randomization is insufficient for ensuring the robustness of motion policies, and that attack policies can effectively identify the vulnerabilities of motion policies and add more powerful perturbation effects.

TABLE II
ROBUSTNESS ANALYSIS OF PERCEPTIVE LOCOMOTION POLICIES

Environments	Policies	Metrics		
		$E_{vel}(m/s)$	$E_{ang}(rad/s)$	$E_g(m/s^2)$
CE	PL-DR	0.206	0.289	0.329
	PL-CAP	0.195	0.247	0.301
DR	PL-DR	0.212	0.339	0.422
	PL-CAP	0.204	0.324	0.406

2) *Robustness of Motion Policies*: We compare the performance of motion policies trained by different methods in clean environments without perturbations and in domain randomized environments with perturbations, respectively. In the perceptive locomotion task, we evaluate velocity tracking performance E_{vel} , E_{ang} and the gravitational projection component E_g of motion policies on flat ground, slopes, stairs, and discrete terrains. As shown in Table II, compared to PL-DR, PL-CAP achieves better performance indicators regardless of the presence of perturbations. This indicates that adversarial training can significantly compensate for the vulnerability of motion policies and improve their performance and robustness against perturbations. For the whole-body control task, we analyze the trajectory tracking performance of the motion policies, as shown in Fig. 3. The WBC-CAP is significantly superior to the WBC-DR in multiple trajectory tracking indicators, especially the velocity tracking indicators E_{vel} , E_{ang} . The results demonstrate that WBC-CAP has a higher self-stabilization ability and imitation ability during the trajectory tracking process, avoiding the sacrifice of trajectory tracking accuracy for maintaining self-stability.

3) *Ablation Study*: To evaluate the impact of CAP on the performance of motion policies, we compare the performance of motion policies trained adversarially by PAP and CAP under different attack threshold conditions. In the simulation, we defined the perturbation level as $L_p \in \{1, 2, 3, 4\}$, where the attack threshold is scaled by L_p . In each L_p environment, perceptive locomotion policies are trained adversarially using PAP and CAP, denoted as PL-PAP- L_p and PL-CAP- L_p , respectively, and the normalized rewards after sufficient training are recorded, as shown in Fig. 4(a). Compared with the domain randomization method, the adversarial training method can effectively improve the robustness of the motion policy. In addition, as the perturbation level L_p increases, normalized rewards of PL-CAP- L_p decrease less than that of PL-PAP- L_p . This is because CAP only imposes attacks on the vulnerable states of the motion policy, avoiding the excessive conservatism of the motion policy caused by many invalid attacks in stable states. To further verify this conclusion, we compare the performance of adversarially trained motion policies under different perturbation levels L_p in unperturbed environments, as shown in Fig. 4(b). The performance of PL-CAP- L_p degrades more slowly, while the performance degradation of PL-PAP- L_p exceeds that of PL-DR. The experimental results show that PAP has stronger attack capabilities, but the full-time attack causes

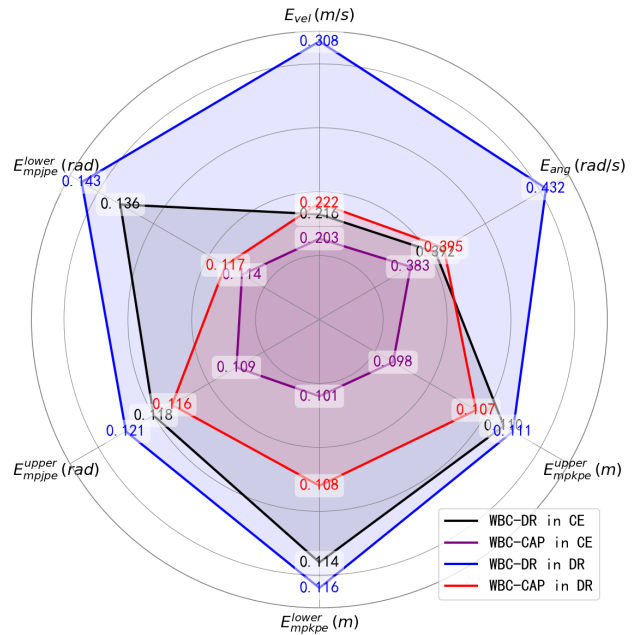


Fig. 3. Performance analysis of whole body control. The trajectory tracking errors of WBC-DR and WBC-CAP are evaluated in clean environments without perturbations and in domain randomized environments with perturbations. The WBC-CAP has smaller tracking errors in all indicators, indicating that adversarial training significantly improves the stability of the WBC policy, thereby improving tracking performance.

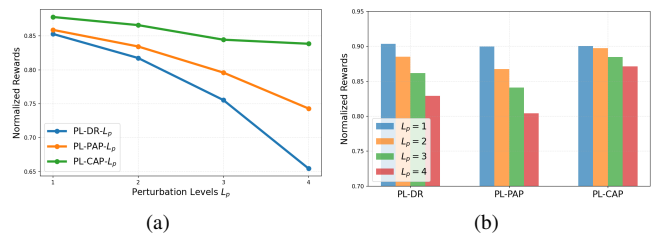


Fig. 4. Comparative experiment on the impact of different attack policies on the performance of motion policies. (a) Rewards of motion policies learned based on different attack policies under different perturbation levels L_p . (b) Performance comparison of motion policies trained based on different perturbation levels L_p in unperturbed environments.

a significant state distribution shift in the state of the motion policy, resulting in a significant decrease in the performance of the motion policy in low-perturbation environments. In contrast, CAP only attacks the vulnerable states of the motion policy, featuring certain high efficiency and stealthiness, and effectively balances the motion performance of the motion policy and the robustness against perturbations.

4) *Analysis of Critical Attack Policy*: We evaluate the attack ratio of the CAP in different motion tasks, as illustrated in Fig. 5. For perceptive locomotion tasks, the attack ratio is tested on flat, slopes, stairs, and discrete terrain. In whole-body control tasks, the tracking trajectories are categorized into simple walking trajectories and dancing trajectories requiring enhanced dynamic balance, with attack ratios measured separately for each category. The experimental results show that as the difficulty of the task increases, the attack ratio also increases, reflecting that CAP has learned to

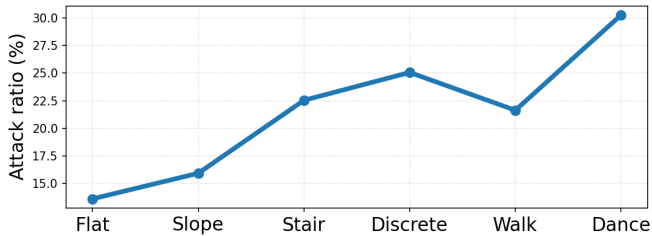


Fig. 5. The attack ratio of CAP in one episode under different motion tasks. In simple terrain, the robot state is relatively stable, resulting in a low attack ratio of CAP. As the terrain difficulty increases, the attack ratio gradually increases. In trajectory imitation tasks, the attack ratio is higher in dancing trajectory imitation.

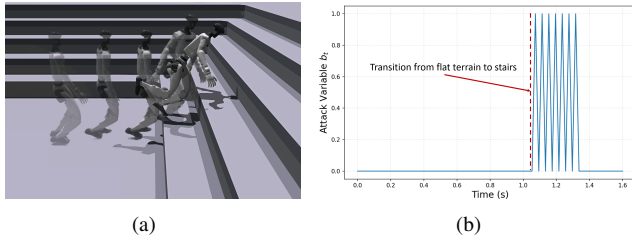


Fig. 6. Demonstration of CAP attack sequences during the robot transitions from flat terrain to stairs. (a) Visualization of robot motion states. (b) Attack variable sequence. The robot maintains relatively stable motion on flat terrain, with no attacks imposed by CAP. However, as the robot prepares to ascend the stairs, CAP identifies the vulnerability of this motion state and applies a small number of attacks, which successfully attack the motion policy and cause the robot to fall.

impose targeted attacks. In addition, we specifically analyze the attack behavior of CAP during the robot’s transition from flat terrain to stairs. As shown in Fig. 6, when moving on flat terrain, the motion policy is not perturbed due to the good stability of the robot body. However, during the robot’s transition from flat terrain to stairs, the attack policy identifies the vulnerability of this state and imposed a small number of perturbation attacks to force the robot to fall, indicating that CAP can significantly distinguish the differences in vulnerability between different motion states of the robot and impose perturbation attacks in a targeted manner, thereby forcing the motion policy to continuously compensate for the vulnerable state in adversarial training and improve robustness.

5) *Analyzing Hyperparameter λ* : In CAP training, the hyperparameter λ is used to regulate the frequency of adversarial attacks. We perform a comparative analysis of the attack ratio and motion performance of the WBC-CAP under different λ in adversarial training. As illustrated in Fig. 7, as the parameter λ increases, the attack ratio decreases significantly. However, the motion performance of the WBC-CAP exhibits a trend of increasing first and then decreasing. When λ increases from 10^{-3} to 10^{-1} , CAP learns to identify vulnerabilities in different motion states of the robot while reducing the attack ratio, thereby improving attack efficiency and enhancing the robustness of the motion policy. However, when λ further increases from 10^{-1} to 10^1 , the excessive penalty on attack number leads to a severe reduction in the attack ratio. Consequently, CAP fails to apply targeted

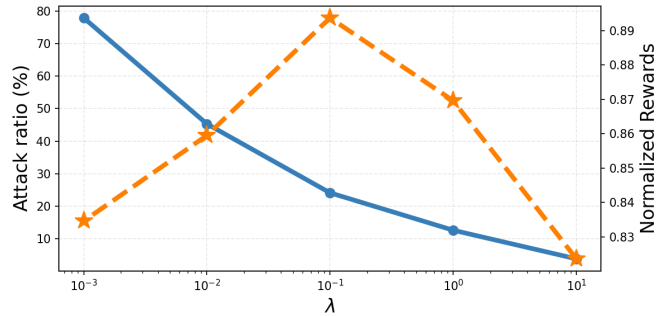


Fig. 7. Compare the attack ratio and performance of WBC-CAP with respect to the parameter λ . The blue line represents the attack ratio and the orange line represents the reward. As λ increases, the attack ratio decreases, but the performance shows a trend of first increasing and then decreasing. This indicates the necessity of adversarial attacks, but untargeted attacks are not conducive to improving the robustness of motion policies, thereby requiring an effective balance between attack strength and task performance.

adversarial attacks effectively, resulting in insufficient adversarial strength during training, and the motion policy cannot effectively improve its own robustness. Therefore, in adversarial training for specific tasks, the parameter λ needs to be carefully designed to effectively balance attack strength and task performance.

C. Real-World Experiments

1) *Complex Terrain Traversability*: To evaluate the terrain traversability of PL-CAP, we build a standardized testing environment encompassing various challenging terrains, including stairs, slopes, gravel, sands, and grass, as shown in Fig. 8. We perform comparative tests on the terrain traversal success rates between PL-DR and PL-CAP. Each terrain is tested 20 times, and the number of successes is recorded. The experimental results are illustrated in Table III. Benefiting from the effective identification of vulnerabilities in the motion policy and the application of critical adversarial perturbations, the adversarially trained PL-CAP demonstrates significantly enhanced locomotion performance on the real robot. Fig. 8 shows snapshots of our method traversing complex terrains. In the tests on stairs and slopes terrains, the frequency of foot tripping and slipping of PL-CAP is significantly reduced compared to PL-DR. In addition, the ridges in the terrain connection area are thin and sparsely distributed, making it difficult for the elevation map to perceive them. PL-DR often falls due to tripping at the terrain connection. In contrast, PL-CAP can effectively adapt to this complex terrain and maintain body stability. The experimental results demonstrate that the proposed method effectively enhances the robustness of locomotion policies, validating the critical role of adversarial training in the co-optimization of complex environment perception and motion control.

2) *Whole-Body Trajectory Imitation Performance*: We further evaluate the performance of the whole-body control on the real robot by tracking 48 seconds of dynamic dance motion. The two joint trajectory tracking indicators E_{mpjpe}^{lower} and E_{mpjpe}^{upper} are tested, as shown in Fig. 9. Due to the

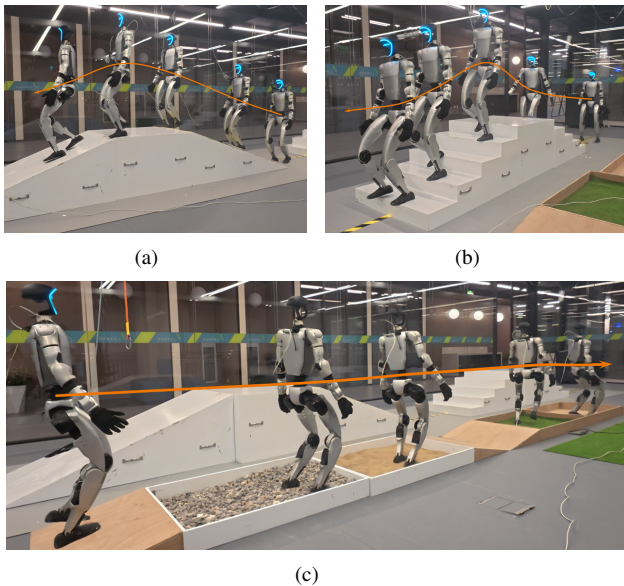


Fig. 8. Evaluating the motion performance of PL-CAP in traversing complex terrain. (a) The robot traverses 30° slopes. (b) The robot traverses 16 cm stairs. (c) The robot traverses gravel and sandy terrain. PL-CAP significantly improves the success rate of terrain traversal, indicating the robustness of the motion policy.

TABLE III
SUCCESS RATES OF COMPLEX TERRAIN TRAVERSAL

Policies	Terrains				
	Slopes	Stairs	Gravel	Sands	Grass
PL-DR	55%	45%	70%	70%	80%
PL-CAP	90%	85%	90%	90%	95%

high dynamic balancing demands of the dance trajectory, WBC-DR exhibits progressively accumulating tracking errors, ultimately causing instability and premature termination after only 26 seconds of execution. In contrast, WBC-CAP effectively mitigates temporal composite tracking errors and successfully completes the 48-second motion trajectory. Snapshot of the imitation of dance motions are presented in Fig. 1, demonstrating the robot’s ability to dynamically regulate the balance of the whole body while performing complex trajectory tracking. These results indicate that adversarial training significantly enhances the robustness of motion policies and effectively bridges the sim-to-real gap in dynamic motion control.

VI. CONCLUSION

This paper proposes a novel robust adversarial training paradigm, aiming to address the sim-to-real gap and enhance the robustness of RL-based motion policies for humanoid robots. By introducing the critical attack policy, which is capable of identifying vulnerable states and imposing targeted perturbations under constrained attack costs, the motion policies are strengthened through dynamic non-zero-sum game optimization. Extensive experiments conducted on the Unitree G1 humanoid robot have verified the superiority of adversarial training. Future work will explore potential

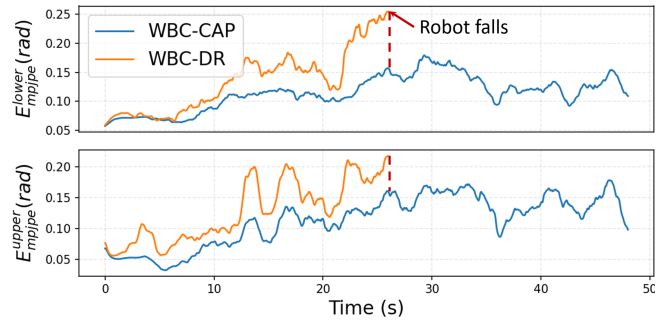


Fig. 9. The Mean Per Joint Position Error of each frame in the dance trajectory imitation. Due to the insufficient robustness of PL-DR, the robot loses balance and terminates prematurely at 26 seconds. PL-CAP effectively reduces the trajectory tracking error and improves the robustness of the whole-body control.

perturbation attacks in the interaction between robots and the environment, so as to enhance the adaptability of robots to dynamic environments. In addition, optimizing the attack cost constraint mechanism to further refine the trade-off between attack efficacy and policy agility remains a promising direction.

REFERENCES

- [1] Z. Gu, J. Li, W. Shen, W. Yu, Z. Xie, S. McCrory, X. Cheng, A. Shamsah, R. Griffin, C. K. Liu *et al.*, “Humanoid locomotion and manipulation: Current progress and challenges in control, planning, and learning,” *arXiv preprint arXiv:2501.02116*, 2025.
- [2] Y. Tong, H. Liu, and Z. Zhang, “Advancements in humanoid robots: A comprehensive review and future prospects,” *IEEE/CAA Journal of Automatica Sinica*, vol. 11, no. 2, pp. 301–328, 2024.
- [3] M. Mende, M. L. Scott, J. Van Doorn, D. Grewal, and I. Shanks, “Service robots rising: How humanoid robots influence service experiences and elicit compensatory consumer responses,” *Journal of Marketing Research*, vol. 56, no. 4, pp. 535–556, 2019.
- [4] A. A. Malik, T. Masood, and A. Brem, “Intelligent humanoids in manufacturing to address worker shortage and skill gaps: Case of tesla optimus,” *arXiv preprint arXiv:2304.04949*, 2023.
- [5] S. Mukherjee, M. M. Baral, S. K. Pal, V. Chittipaka, R. Roy, and K. Alam, “Humanoid robot in healthcare: a systematic review and future research directions,” in *2022 International conference on machine learning, big data, cloud and parallel computing (COM-IT-CON)*, vol. 1. IEEE, 2022, pp. 822–826.
- [6] X. Gu, Y.-J. Wang, X. Zhu, C. Shi, Y. Guo, Y. Liu, and J. Chen, “Advancing humanoid locomotion: Mastering challenging terrains with denoising world model learning,” *arXiv preprint arXiv:2408.14472*, 2024.
- [7] Z. Fu, Q. Zhao, Q. Wu, G. Wetzstein, and C. Finn, “Humanplus: Humanoid shadowing and imitation from humans,” *arXiv preprint arXiv:2406.10454*, 2024.
- [8] A. Tang, T. Hiraoka, N. Hiraoka, F. Shi, K. Kawaharazuka, K. Kojima, K. Okada, and M. Inaba, “Humanmimic: Learning natural locomotion and transitions for humanoid robot via wasserstein adversarial imitation,” in *2024 IEEE International Conference on Robotics and Automation (ICRA)*. IEEE, 2024, pp. 13 107–13 114.
- [9] T. He, Z. Luo, W. Xiao, C. Zhang, K. Kitani, C. Liu, and G. Shi, “Learning human-to-humanoid real-time whole-body teleoperation,” in *2024 IEEE/RSJ International Conference on Intelligent Robots and Systems (IROS)*. IEEE, 2024, pp. 8944–8951.
- [10] C. Zhang, W. Xiao, T. He, and G. Shi, “Wococo: Learning whole-body humanoid control with sequential contacts,” *arXiv preprint arXiv:2406.06005*, 2024.
- [11] W. Wei, Z. Wang, A. Xie, J. Wu, R. Xiong, and Q. Zhu, “Learning gait-conditioned bipedal locomotion with motor adaptation,” in *2023 IEEE-RAS 22nd International Conference on Humanoid Robots (Humanoids)*. IEEE, 2023, pp. 1–7.

- [12] Z. Chen, X. He, Y.-J. Wang, Q. Liao, Y. Ze, Z. Li, S. S. Sastry, J. Wu, K. Sreenath, S. Gupta *et al.*, "Learning smooth humanoid locomotion through lipschitz-constrained policies," *arXiv preprint arXiv:2410.11825*, 2024.
- [13] K. Yamamoto, T. Kamioka, and T. Sugihara, "Survey on model-based biped motion control for humanoid robots," *Advanced Robotics*, vol. 34, no. 21-22, pp. 1353–1369, 2020.
- [14] I. Radosavovic, T. Xiao, B. Zhang, T. Darrell, J. Malik, and K. Sreenath, "Real-world humanoid locomotion with reinforcement learning," *Science Robotics*, vol. 9, no. 89, p. eadi9579, 2024.
- [15] X. Gu, Y.-J. Wang, and J. Chen, "Humanoid-gym: Reinforcement learning for humanoid robot with zero-shot sim2real transfer," *arXiv preprint arXiv:2404.05695*, 2024.
- [16] I. Radosavovic, B. Zhang, B. Shi, J. Rajasegaran, S. Kamat, T. Darrell, K. Sreenath, and J. Malik, "Humanoid locomotion as next token prediction," in *The Thirty-eighth Annual Conference on Neural Information Processing Systems*, 2024.
- [17] Z. Zhuang, S. Yao, and H. Zhao, "Humanoid parkour learning," *arXiv preprint arXiv:2406.10759*, 2024.
- [18] J. Long, J. Ren, M. Shi, Z. Wang, T. Huang, P. Luo, and J. Pang, "Learning humanoid locomotion with perceptive internal model," *arXiv preprint arXiv:2411.14386*, 2024.
- [19] B. van Marum, A. Shrestha, H. Duan, P. Dugar, J. Dao, and A. Fern, "Revisiting reward design and evaluation for robust humanoid standing and walking," *arXiv preprint arXiv:2404.19173*, 2024.
- [20] M. Ji, X. Peng, F. Liu, J. Li, G. Yang, X. Cheng, and X. Wang, "Exbody2: Advanced expressive humanoid whole-body control," *arXiv preprint arXiv:2412.13196*, 2024.
- [21] Q. Zhang, P. Cui, D. Yan, J. Sun, Y. Duan, G. Han, W. Zhao, W. Zhang, Y. Guo, A. Zhang *et al.*, "Whole-body humanoid robot locomotion with human reference," in *2024 IEEE/RSJ International Conference on Intelligent Robots and Systems (IROS)*. IEEE, 2024, pp. 11 225–11 231.
- [22] T. Fujimoto, J. Suetterlein, S. Chatterjee, and A. Ganguly, "Assessing the impact of distribution shift on reinforcement learning performance," *arXiv preprint arXiv:2402.03590*, 2024.
- [23] Y. Liang, Y. Sun, R. Zheng, and F. Huang, "Efficient adversarial training without attacking: Worst-case-aware robust reinforcement learning," *Advances in Neural Information Processing Systems*, vol. 35, pp. 22 547–22 561, 2022.
- [24] X. B. Peng, M. Andrychowicz, W. Zaremba, and P. Abbeel, "Sim-to-real transfer of robotic control with dynamics randomization," in *2018 IEEE international conference on robotics and automation (ICRA)*. IEEE, 2018, pp. 3803–3810.
- [25] J. Moos, K. Hansel, H. Abdulsamad, S. Stark, D. Clever, and J. Peters, "Robust reinforcement learning: A review of foundations and recent advances," *Machine Learning and Knowledge Extraction*, vol. 4, no. 1, pp. 276–315, 2022.
- [26] T. Kobayashi, "L2c2: Locally lipschitz continuous constraint towards stable and smooth reinforcement learning," in *2022 IEEE/RSJ International Conference on Intelligent Robots and Systems (IROS)*. IEEE, 2022, pp. 4032–4039.
- [27] Y. Tang, J. Tan, and T. Harada, "Learning agile locomotion via adversarial training," in *2020 IEEE/RSJ International Conference on Intelligent Robots and Systems (IROS)*. IEEE, 2020, pp. 6098–6105.
- [28] F. Shi, C. Zhang, T. Miki, J. Lee, M. Hutter, and S. Coros, "Rethinking robustness assessment: Adversarial attacks on learning-based quadrupedal locomotion controllers," *arXiv preprint arXiv:2405.12424*, 2024.
- [29] S. Huang, N. Papernot, I. Goodfellow, Y. Duan, and P. Abbeel, "Adversarial attacks on neural network policies," *arXiv preprint arXiv:1702.02284*, 2017.
- [30] H. Zhang, H. Chen, D. Boning, and C.-J. Hsieh, "Robust reinforcement learning on state observations with learned optimal adversary," *arXiv preprint arXiv:2101.08452*, 2021.
- [31] C. Tessler, Y. Efroni, and S. Mannor, "Action robust reinforcement learning and applications in continuous control," in *International Conference on Machine Learning*. PMLR, 2019, pp. 6215–6224.
- [32] Y. Kuang, M. Lu, J. Wang, Q. Zhou, B. Li, and H. Li, "Learning robust policy against disturbance in transition dynamics via state-conservative policy optimization," in *Proceedings of the AAAI Conference on Artificial Intelligence*, vol. 36, no. 7, 2022, pp. 7247–7254.
- [33] Unitree G1, <https://www.unitree.com/cn/g1>, 2025, [Online; accessed 25-June-2025].
- [34] J. Ren, T. Huang, H. Wang, Z. Wang, Q. Ben, J. Pang, and P. Luo, "Vbcom: Learning vision-blind composite humanoid locomotion against deficient perception," *arXiv preprint arXiv:2502.14814*, 2025.
- [35] W. Cui, S. Li, H. Huang, B. Qin, T. Zhang, L. Zheng, Z. Tang, C. Hu, N. Yan, J. Chen *et al.*, "Adapting humanoid locomotion over challenging terrain via two-phase training," in *8th Annual Conference on Robot Learning*.
- [36] X. Cheng, Y. Ji, J. Chen, R. Yang, G. Yang, and X. Wang, "Expressive whole-body control for humanoid robots," *arXiv preprint arXiv:2402.16796*, 2024.
- [37] P. Dugar, A. Shrestha, F. Yu, B. van Marum, and A. Fern, "Learning multi-modal whole-body control for real-world humanoid robots," *arXiv preprint arXiv:2408.07295*, 2024.
- [38] A. Kumar, Z. Fu, D. Pathak, and J. Malik, "Rma: Rapid motor adaptation for legged robots," *arXiv preprint arXiv:2107.04034*, 2021.
- [39] Z. Wang, W. Wei, R. Yu, J. Wu, and Q. Zhu, "Toward understanding key estimation in learning robust humanoid locomotion," *arXiv preprint arXiv:2403.05868*, 2024.
- [40] H. Zhang, L. Zhang, Z. Chen, L. Chen, Y. Wang, and R. Xiong, "Natural humanoid robot locomotion with generative motion prior," *arXiv preprint arXiv:2503.09015*, 2025.
- [41] H. Wang, Z. Wang, J. Ren, Q. Ben, T. Huang, W. Zhang, and J. Pang, "Beamdojo: Learning agile humanoid locomotion on sparse footholds," *arXiv preprint arXiv:2502.10363*, 2025.
- [42] W. Sun, B. Cao, L. Chen, Y. Su, Y. Liu, Z. Xie, and H. Liu, "Learning perceptive humanoid locomotion over challenging terrain," *arXiv preprint arXiv:2503.00692*, 2025.
- [43] T. He, W. Xiao, T. Lin, Z. Luo, Z. Xu, Z. Jiang, J. Kautz, C. Liu, G. Shi, X. Wang *et al.*, "Hover: Versatile neural whole-body controller for humanoid robots," *arXiv preprint arXiv:2410.21229*, 2024.
- [44] Y. Ze, Z. Chen, J. P. Arasjo, Z.-a. Cao, X. B. Peng, J. Wu, and C. K. Liu, "Twist: Teleoperated whole-body imitation system," *arXiv preprint arXiv:2505.02833*, 2025.
- [45] X. He, R. Dong, Z. Chen, and S. Gupta, "Learning getting-up policies for real-world humanoid robots," *arXiv preprint arXiv:2502.12152*, 2025.
- [46] T. He, J. Gao, W. Xiao, Y. Zhang, Z. Wang, J. Wang, Z. Luo, G. He, N. Sobanbab, C. Pan *et al.*, "Asap: Aligning simulation and real-world physics for learning agile humanoid whole-body skills," *arXiv preprint arXiv:2502.01143*, 2025.
- [47] J. Wang, Y. Liu, and B. Li, "Reinforcement learning with perturbed rewards," in *Proceedings of the AAAI conference on artificial intelligence*, vol. 34, no. 04, 2020, pp. 6202–6209.
- [48] J. Shi, X. Liu, D. Wang, O. Lu, S. Schwertfeger, F. Sun, C. Bai, and X. Li, "Adversarial locomotion and motion imitation for humanoid policy learning," *arXiv preprint arXiv:2504.14305*, 2025.
- [49] Y. Zhang, B. Nie, and Y. Gao, "Robust locomotion policy with adaptive lipschitz constraint for legged robots," *IEEE Robotics and Automation Letters*, 2024.
- [50] S. Mysore, B. Mabsout, R. Mancuso, and K. Saenko, "Regularizing action policies for smooth control with reinforcement learning," in *2021 IEEE International Conference on Robotics and Automation (ICRA)*. IEEE, 2021, pp. 1810–1816.
- [51] N. Cho and Y. Kim, "On the stability of lipschitz continuous control problems and its application to reinforcement learning," *arXiv preprint arXiv:2404.13316*, 2024.
- [52] N. H. Barbara, R. Wang, and I. R. Manchester, "On robust reinforcement learning with lipschitz-bounded policy networks," *arXiv preprint arXiv:2405.11432*, 2024.
- [53] W. Guo, X. Wu, S. Huang, and X. Xing, "Adversarial policy learning in two-player competitive games," in *International conference on machine learning*. PMLR, 2021, pp. 3910–3919.
- [54] J. Perolat, B. Scherrer, B. Piot, and O. Pietquin, "Approximate dynamic programming for two-player zero-sum markov games," in *International Conference on Machine Learning*. PMLR, 2015, pp. 1321–1329.
- [55] F. G. Harvey, M. Yurick, D. Nowrouzezahrai, and C. Pal, "Robust motion in-betweening," *ACM Transactions on Graphics (TOG)*, vol. 39, no. 4, pp. 60–1, 2020.